Spring 5-1-2021

Soil Inhomogeneity Effects on Seismic Wind Noise

Bipin Koirala
University of Mississippi

SOIL INHOMOGENEITY EFFECTS ON SEISMIC WIND NOISE

by
Bipin Koirala

A thesis submitted to the faculty of The University of Mississippi in partial fulfillment of the requirements of the Sally McDonnell Barksdale Honors College.

Oxford
May 2021

Advisor: Dr. Richard Raspet

Reader: Dr. Farhad Farzbod

Reader: Dr. Likun Zhang

ACKNOWLEDGEMENTS

I would like to express my deepest appreciation to my thesis advisor Dr. Richard Raspet for his unparalleled support, guidance, and profound belief in my ability to bring this thesis to fruition. It has been a greatly enriching experience for me to work under his supervision. I would also like to extend my sincere thanks to Dr. Farhaz Farzbod and Dr. Likun Zhang for serving as committee members and providing invaluable suggestions to improve my thesis.

Special thanks to Sally McDonnell Barksdale Honors College, Department of Mechanical Engineering, and National Center for Physical Acoustics (NCPA) at the University of Mississippi for providing me with the opportunity to write an undergraduate thesis.

Finally, I would like to thank my parents, Mr. Uma Kanta Koirala and Mrs. Kalpana Tiwari Koirala, for their unyielding love, support and encouragement throughout my study.

Abstract

Wind causes local pressure fluctuations over the ground. The pressure waves couples with the ground and transmits into the ground as seismic waves. The seismic wave, in turn, causes ground motion. Naderyan et al. [9] developed a prediction of the ground displacements spectra from the measured ground properties and predicted pressure and shear stress at the ground surface. Naderyan modeled the ground as a linearly elastic half space bounded by an infinite plane on one side. The quasi-static model for predicting displacement components in the ground is effective for the vertical component of the displacement response, but the model significantly underpredicted the horizontal component. In this paper, the displacement response of a half space bounded by a low shear strength surface layer and a high compression speed layer at 0.5 m depth is investigated. The addition of a water-saturated layer as the bottom half space showed an improved prediction in the horizontal displacement of the ground.. The inhomogeneity of the ground was modeled by subdividing the intermediate layer between the low shear velocity layer and a water table to ten discrete layers with randomly varying parameters. Introducing inhomogeneity in the ground model did not improve the prediction for the displacement response of the ground.

Contents

List of Figures

1 Introduction

Seismologists rely on measuring seismic waves for locating earthquakes, for fossil fuel exploration, for monitoring volcanic activities and to study the earth's structure. Wind causes velocity changes over the ground which result in pressure fluctuations on the surface which in turn induce seismic motion in the ground. The localized pressure fluctuation perturbations on the ground surface are a source of seismic motion. This phenomenon poses a difficulty with infrasonic measurements and affects the measurement recorded by a sensor deployed at or near the surface of the earth.

The quasi-static model adopted by Naderyan et al. [9] does not correctly predict the vertical to horizontal displacement ratio of the ground as depth varies. This paper aims to include the theory behind the coupling of slow moving plane pressure fluctuations into vertical and horizontal ground displacement motion in a homogeneous elastic half space as presented by Sorrells [13]. Furthermore, the acoustic-seismic coupling theory is used to obtain the displacement response of an elastic half-space and a multi-layered inhomogeneous elastic media. The multi-layer media consists of ten separate layers, with stochastic layer parameters, sandwiched between a soft shear layer near the surface and a water table as the lower half space. This paper also investigates the effectiveness of acoustic-seismic coupling theory in predicting the displacements as a function of depth in an inhomogeneous ground.

Section 2 includes the necessary theory behind acoustic to seismic coupling using Sorrells[13] wave model and also discusses the improved version of the transfer matrix method, by Lévesque and Piché [6], used to propagate shear stress and displacements across multilayered media. Section 3 investigates the displacement response of an elastic half space, similar to Naderyan et al. [9] model, and discusses the limitation of quasi-static model on predicting ground response. Section 4 studies the predicted displacement components for a multilayer inhomogeneous ground conditions. Section 5 presents the conclusions of the study.

2 Theory

2.1 Acoustic to Seismic Coupling

As stated in Section 1, wind poses difficulty in measurement of seismic waves, especially if the sensor is deployed near the surface of the earth. It is therefore required to have an understanding of how a plane pressure wave, generated as a result of pressure fluctuation due to wind, couples with an elastic media and results in its elastic deformation.

2.2 Displacement Response of an Elastic Half-Space

The coupling of a plane pressure wave into a homogeneous elastic half space is presented in this section. Setup for the theory is same as Raspet et al. [10] which follows Sorrells [13] in the notation of Brekhovskikh [1].

Let x and z be the Cartesian co-ordinates in directions parallel to the wind and perpendicular to the surface of the medium respectively. The normal component z denotes the depth into the ground. The displacement solution can be expressed in terms of a compression potential and a shear potential. These potentials obey the wave equation as:

$$\nabla^2\varphi = \frac{1}{\alpha^2}\left(\frac{\partial^2\varphi}{\partial t^2}\right) \tag{1}$$

$$\nabla^2\psi = \frac{1}{\beta^2}\left(\frac{\partial^2\psi}{\partial t^2}\right) \tag{2}$$

where α and β are compression and shear wave speed respectively.

A wind moving at a speed c creates pressure fluctuations in local space over the ground and the speed of propagation of pressure is given by the convection velocity, which is usually taken as 0.7 times the average wind speed at 2.0 m above the ground surface. The wave number (horizontal component) is given by $k = \frac{\omega}{c}$ where angular frequency $\omega = 2\pi f$ where f is the wave frequency.

For simplification purpose, P_o is taken as unit pressure field and the pressure wave is given by:

$$P(x,t) = P_o \; e^{i(kx-\omega t)} \tag{3}$$

Where a harmonic time dependence $e^{-i\omega t}$ is assumed. The harmonic excitation represented by (3) gives compression wave (4) and shear wave (5) in the medium:

$$\varphi = \varphi_o \; e^{-\gamma z} \; e^{i(kx-\omega t)} \tag{4}$$

$$\psi = \psi_o \; e^{-\delta z} \; e^{i(kx-\omega t)} \tag{5}$$

Equations (4) & (5) suggest that the shear potential and compression potential decrease exponentially with the increase in depth for a given homogeneous medium. Here, δ and γ give the attenuation in z direction for shear and compression wave respectively.

$$\delta = \sqrt{k^2 - \left(\frac{\omega}{\beta}\right)^2} \tag{6}$$

$$\gamma = \sqrt{k^2 - \left(\frac{\omega}{\alpha}\right)^2} \tag{7}$$

Harmonic pressure waves with the dependence of all quantities on time t and the coordinate x in the form of $e^{i(kx-wt)}$ are considered throughout this paper. Since, horizontal wave number k is conserved in the transition through the interface; $\frac{\partial}{\partial x} = i \; k$ and $\frac{\partial}{\partial t} = -i \; \omega$.

In general, the displacement vector $\vec{a}$ can be expressed in terms of scalar φ and vector ψ.

$$\vec{a} = \nabla\varphi + \nabla \times \vec{\psi} \tag{8}$$

We now obtain horizontal displacement u and vertical displacement w as:

$$u = ik\varphi - \left(\frac{\partial \psi}{\partial z}\right) \tag{9}$$

$$w = ik\psi + \left(\frac{\partial \varphi}{\partial z}\right) \tag{10}$$

The final expression for displacement response of an elastic half space at depth z due to plane pressure wave near the surface of the ground.

$$u = \left(i\ \varphi_o\ k\ e^{-\gamma z}\ +\ \psi_o\ \delta\ e^{-\delta z}\right) \times e^{i(kx-\omega t)} \tag{11}$$

$$w = \left(-\varphi_o\ \gamma\ e^{-\gamma z}\ +\ i\ \psi_o\ k\ e^{-\delta z}\right) \times e^{i(kx-\omega t)} \tag{12}$$

u and w are the displacement components in positive x and z direction inside the elastic half-space. The components of displacement vector should be continuous in penetration of the interface and the components of stress tensor should be continuous at the boundary.

$$Z_z = \lambda\ \left(\frac{\partial u}{\partial x} + \frac{\partial w}{\partial z}\right) + 2\mu \left(\frac{\partial w}{\partial z}\right) \tag{13}$$

$$Z_x = \mu\ \left(\frac{\partial u}{\partial z} + \frac{\partial w}{\partial x}\right) \tag{14}$$

$$Z_y = 0\ (from\ setup). \tag{15}$$

Here; λ and μ are Lamé parameters. If ρ is the density of an elastic medium, the Lamé parameters are given in terms of wave speed by:

$$\lambda = \rho\ \left(\alpha^2 - 2\beta^2\right) \tag{16}$$

$$\mu = \beta^2 \rho \tag{17}$$

Following continuity of displacement and stress criteria remains valid on the boundaries of separation of media in order to facilitate a smooth propagation of wave. $[Z_z] = 0$ and $[Z_x] = 0$. "[ ]", represents difference across the boundary between any two media. According to the coordinate setup, we get:

$$Z_z = -P_o \, e^{i(kx-wt)} \, |_{z=0} \; ; \tag{18}$$

$$Z_x = 0 \, |_{z=0} \tag{19}$$

Figure 1 shows a plane pressure harmonic wave propagating near the surface of the earth and coupling with the ground, causing a displacement response of the ground in both horizontal and vertical directions. The wave in the ground is elliptically polarized with a phase difference of between displacements which varies with depth and the wave amplitude decays exponentially with the increase in depth.

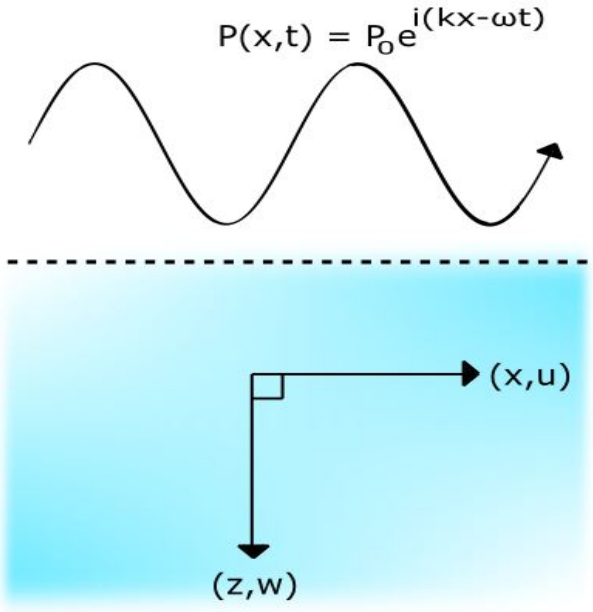

Figure 1: Displacement response of elastic half space due to plane pressure wave above the ground [10]

2.3 Displacement Response of a Multi-layer Elastic Media

Previous sections explicitly deal with a homogeneous half space. This section investigates the displacement response of a multi-layer elastic media and develops the theory to obtain the vertical displacement and horizontal displacement. Determining the displacement response at an arbitrary depth z, below the ground, for a multi-layer media requires a different approach and is not as simple as the case of a homogeneous elastic half-space. Thomson [14] and Haskell [4] proposed a matrix method that transfers stress and displacement across the interfaces as a systematic approach to evaluating acoustic propagation in multilayered systems.

Figure 3 shows an elastic medium with a discrete number of layer ranging from 1^{st} to n^{th}. The region above Z_0 is the atmosphere and the region below Z_n is considered to be a water-saturated layer. A plane pressure wave due to wind passes just above Z_0, couples with the elastic media and causes displacement response within the media at any given depth Z.

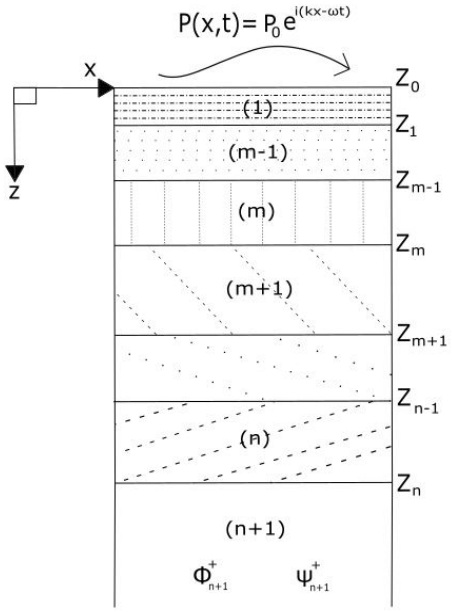

Figure 2: Geometry of multi-layered elastic media

Note: To eliminate any possible confusion, Lévesque and Piché's [6] use of ξ for wave number is adopted, instead of k.

Since the medium is multi-layer, the compression potential (4) and the shear potential (5) now include both the upwards (-) and downwards (+) coefficients. The set of compression potential and shear potential vectors for a given layer, at any depth z, consists of following:

$$\varphi = \left({\varphi_o}^+ e^{-\gamma z} + {\varphi_o}^- e^{\gamma z}\right) e^{i(\xi x - \omega t)} \tag{20}$$

$$\psi = \left({\psi_o}^+ e^{-\delta z} + {\psi_o}^- e^{\delta z}\right) e^{i(\xi x - \omega t)} \tag{21}$$

The horizontal displacement (u) and vertical displacement (w) are given by:

$$u = \left(\frac{\partial \varphi}{\partial x} - \frac{\partial \psi}{\partial z}\right) \tag{22}$$

$$w = \left(\frac{\partial \varphi}{\partial z} + \frac{\partial \psi}{\partial x}\right) \tag{23}$$

For rigidly bonded interfaces between layers, there exists continuity in displacements and stresses values. From equations (13), (14), (22) and (23), the boundary condition for interface at depth Z_m between layers (m) and $(m+1)$ are given by

$$u_m(z_m) = u_{m+1}(z_m); \qquad w_m(z_m) = w_{m+1}(z_m) \tag{24}$$

$$Z_z^m(z_m) = Z_z^{m+1}(z_m); \qquad Z_x^m(z_m) = Z_x^{m+1}(z_m) \tag{25}$$

Let z represent the depth such that $z_{m-1} \leq z \leq z_m$. Similar to improved transfer matrix formalism by Lévesque and Piché [6], the following matrix relations are obtained as a basis

for propagating stress and displacements across different layers.

$$\{q_m(z)\} = [T_m]\{p_m(z)\} \tag{26}$$

$$\{p_m(z)\} = [T_m]^{-1}\{q_m(z)\} \tag{27}$$

Here; $q_m(z)$, $[T_m]$ and $p_m(z)$ represent displacement/stress vector, transfer matrix and potential vector respectively for the m^{th} layer at z depth and are given by:

$$q_m(z) = \begin{bmatrix} u \\ w \\ Z_z \\ Z_x \end{bmatrix}; [T_m] = \begin{bmatrix} i\xi & \delta & i\xi & -\delta \\ -\gamma & i\xi & \gamma & i\xi \\ -\Gamma & -i2\mu\xi\delta & -\Gamma & i2\mu\xi\delta \\ -i2\mu\xi\gamma & \Gamma & i2\mu\xi\gamma & \Gamma \end{bmatrix}$$

$$p_m(z) = \begin{bmatrix} \varphi_o^+ \\ \psi_o^+ \\ \varphi_o^- \\ \psi_o- \end{bmatrix}; [T_m]^{-1} = \frac{1}{2\ \rho_m\ \omega^2} \begin{bmatrix} i2\mu\xi & \frac{\Gamma}{\gamma} & 1 & \frac{-i\xi}{\gamma} \\ \frac{-\Gamma}{\delta} & i2\mu\xi & \frac{-i\xi}{\delta} & -1 \\ i2\mu\xi & \frac{-\Gamma}{\gamma} & 1 & \frac{i\xi}{\gamma} \\ \frac{\Gamma}{\delta} & i2\mu\xi & \frac{i\xi}{\delta} & -1 \end{bmatrix}$$

where $\Gamma = (\rho\omega^2 - 2\rho\beta^2\xi^2)$

As shown in equation (20) and (21), the exponents $e^{\pm\gamma dm}$ and $e^{\pm\delta dm}$ are responsible for attenuation of displacement/shear components and the conversion of displacement vector from top of m^{th} layer at depth Z_{m-1} to bottom at Z_m i.e. $\{q_m(z_m)\} = [E_m]\{q_m(z_{m-1})\}$. Where;

$$[E_m] = \begin{bmatrix} e^{-\gamma dm} & 0 & 0 & 0 \\ 0 & e^{-\delta dm} & 0 & 0 \\ 0 & 0 & e^{\gamma dm} & 0 \\ 0 & 0 & 0 & e^{\delta dm} \end{bmatrix} \tag{28}$$

Conversely, the displacement at depth Z_{m-1} based on the displacement at depth Z_m is given

by $\{q_m(z_{m-1})\} = [E_m]^{-1}\{q_m(z_m)\}$

$$[E_m]^{-1} = \begin{bmatrix} e^{\gamma dm} & 0 & 0 & 0 \\ 0 & e^{\delta dm} & 0 & 0 \\ 0 & 0 & e^{-\gamma dm} & 0 \\ 0 & 0 & 0 & e^{-\delta dm} \end{bmatrix} \tag{29}$$

Lévesque and Piché[6] show the displacement and stress values at in layer $m-1$ depth Z_{m-1} based on the displacement and stress values at depth Z_m in layer m is given by;

$$\begin{bmatrix} u \\ w \\ Z_z \\ Z_x \end{bmatrix}_{m-1} = [T_m][E_m]^{-1}[T_m]^{-1} \begin{bmatrix} u \\ w \\ Z_z \\ Z_x \end{bmatrix}_m \tag{30}$$

Let $[B_m]$ denote $[T_m][E_m]^{-1}[T_m]^{-1}$. Using (30), the displacement and stress values at depth Z_n can be related to the values at Z_0 as:

$$\begin{bmatrix} u^o \\ w^o \\ P \\ o \end{bmatrix}_0 = [B_1][B_2].....[B_{n-1}][B_n] \begin{bmatrix} u \\ w \\ Z_z \\ Z_x \end{bmatrix}_{z=n} \tag{31}$$

Based on (31), displacement/stress vector at the surface is given in terms of the potentials at depth Z_n by the matrix relation below;

$$\begin{bmatrix} u^o \\ w^o \\ P \\ o \end{bmatrix}_{z=0} = [B_1][B_2].....[B_{n-1}][B_n][T_{n+1}] \begin{bmatrix} \varphi^+ \\ \psi^+ \\ 0 \\ 0 \end{bmatrix}_{n+1} \tag{32}$$

Let [H] denote $[B_1][B_2].....[B_{n-1}][B_n][T_{n+1}]$. Now, (32) can be written as;

$$\begin{bmatrix} u^o \\ w^o \\ P \\ o \end{bmatrix}_{z=0} = [H] \begin{bmatrix} \varphi^+ \\ \psi^+ \\ 0 \\ 0 \end{bmatrix}_{n+1} \tag{33}$$

$[H]$ is a 4×4 matrix and the solution for (33) is:

$$\varphi^+_{n+1} = P \left(\frac{H_{42}}{H_{31}H_{42} - H_{32}H_{41}} \right) \tag{34}$$

$$\psi^+_{n+1} = -P \left(\frac{H_{41}}{H_{31}H_{42} - H_{32}H_{41}} \right) \tag{35}$$

Equations (34) and (35) give the shear potential and compression potential values at the bottom half space. However, numeric difficulties arise in the denominator. Therefore, to improve stability in numeric computation, Dunkin[2] introduced a delta matrix operator $[H]^\Delta$ which consists of 2×2 subdeterminants of $[H]$ i.e. $A^\Delta_{ij} = A^{pq}_{rs}$, where pq and rs = 12, 13, 14, 23, 24 and 34. These numbers correspond to i or j = 1, 2, 3, 4, 5, and 6 respectively.

In our case, the denominator in (34) and (35) is resolved into:

$$H_{31}H_{42} - H_{32}H_{41} = H_{12}^{34} = H_{61}^{\Delta} \tag{36}$$

$H^{\Delta} = B_1^{\Delta}B_2^{\Delta}B_3^{\Delta}.....B_n^{\Delta}T_{n+1}^{\Delta}$; and the B_m^{Δ} can be calculated analytically, eliminating numerical problems with equations (34) and (35).

After computing the values for shear potential and compression potential from (34) and (35), we calculate the displacement/stress at an arbitrary depth $Z_{m-1} < Z < Z_m$ by;

$$\begin{bmatrix} u \\ w \\ Z_z \\ Z_x \end{bmatrix}_{Z_{m-1}<Z<Z_m} = [B_{m(Z_m-Z)}][B_{m+1}].....[B_{n-1}][B_n][T_{n+1}] \begin{bmatrix} \varphi^+ \\ \psi^+ \\ 0 \\ 0 \end{bmatrix}_{n+1} \tag{37}$$

Here;

$$[B_{m(Z_m-Z)}] = [T_m][E_{m(Z_m-Z)}]^{-1}[T_m]^{-1} \tag{38}$$

$[B_{m(Z_m-Z)}]$ transports displacement/stress components from Z_m to an arbitrary depth Z located between Z_{m-1} and Z_m. $[B_{m+1}]$ and other terms in (37) are evaluated for Z_{m+1} and so on.

3 Model I: Half-Space Media

In seismology, the elastic homogeneous half-space is the simplest mathematical model of the structure of the Earth bounded by only one plane surface. The model is large in other dimensions so that only the boundary affects the results. We start with the solutions for a half-space model because they are often the first step in understanding the effects of free surfaces on a seismic system.

Naderyan et al. [9] conducted field measurement on the displacement response of the ground and found out that the vertical component of displacement is in same order of magnitude as the horizontal component for a sensor located at depths of 2.5 cm, 20 cm and 40 cm. The increase in depth did not significantly affect the behavior of ground motion across a wide range of frequency 1-100 Hz. The predicted vertical displacement was in good agreement with the experimental value. However, predicted horizontal displacement was significantly lower in magnitude compared to the experimental data. Furthermore, the predictions for displacement response showed a large decrease in the displacement with depth.

The effect of the burial depth and wind velocity on the displacements showed that the wind noise on the sensor above ground was dominated by the direct interaction of the wind with the sensor [9] . Therefore, this study deals with the displacement response at depths of 0.025 m, 0.2m and 0.4 m to rule out direct wind interference with the sensor.

Figure 4 is developed using equation (28) and (29) to obtain φ_o and ψ_0 for the elastic half-space using MATLAB [7] and then using equations (26), (27) and (34) for evaluating effective horizontal displacement and vertical displacement at various frequencies and depths. Model parameters used in Table 1 for the elastic half-space are same as the model used by Naderyan et al. [9].

Table 1: Model parameter for elastic half-space

Density: ρ (kgm^{-3})	**Shear speed:** β (ms^{-1})	**Compression speed:** α (ms^{-1})
1995	140	285

For this model parameters;

$$\text{Poisson}'\text{s ratio} = \frac{\alpha^2 - \beta^2}{2\left(\alpha^2 - \beta^2\right)} = 0.341$$

$$\text{Young}'\text{s modulus} = \frac{\rho\beta^2\left(3\alpha^2 - 4\beta^2\right)}{\alpha^2 - \beta^2} = 1.048 \times 10^8 Pa$$

We are interested in the displacement response of the elastic half-space at frequencies ranging from 1 Hz to 100 Hz at the location of sensor mounted flushed to the surface (0.025 m) and at moderate depths (0.2 m, 0.40 m) for an average convective velocity of 4.948 m/s. Figure 4 shows apparent ground motion, at different depths, due to harmonic pressure fluctuation on the ground across various frequency range. To maintain the resolution of figure, it is represented in logarithmic scale for frequency as well as for displacement magnitude. Displacement magnitude is expressed as a ratio of displacement per unit pressure amplitude. Horizontal displacement and vertical displacement are denoted by solid line and dotted line respectively.

For a half space, the wave model for predicting ground motion shows that the vertical component of displacement dominates over horizontal component for all frequencies 1-100 Hz for sensor at depth 0.025 m. In case of burial depths at 0.2 m and 0.4 m, it predicts the dominance of vertical component over horizontal only for frequencies below 20 Hz. This displacement behavior is similar to quasi-static model adopted by Nadaryan et al. [9] and does not explicitly agree with the experimental value. Therefore, the wave model for a homogeneous half space is not effective theory to be considered for improving displacement response for an elastic half space. Figure 4 provides an insight to the degree of involvement of wind noise at different depths in the ground. The dips are observed as a result of phase change for horizontal component at certain frequencies.

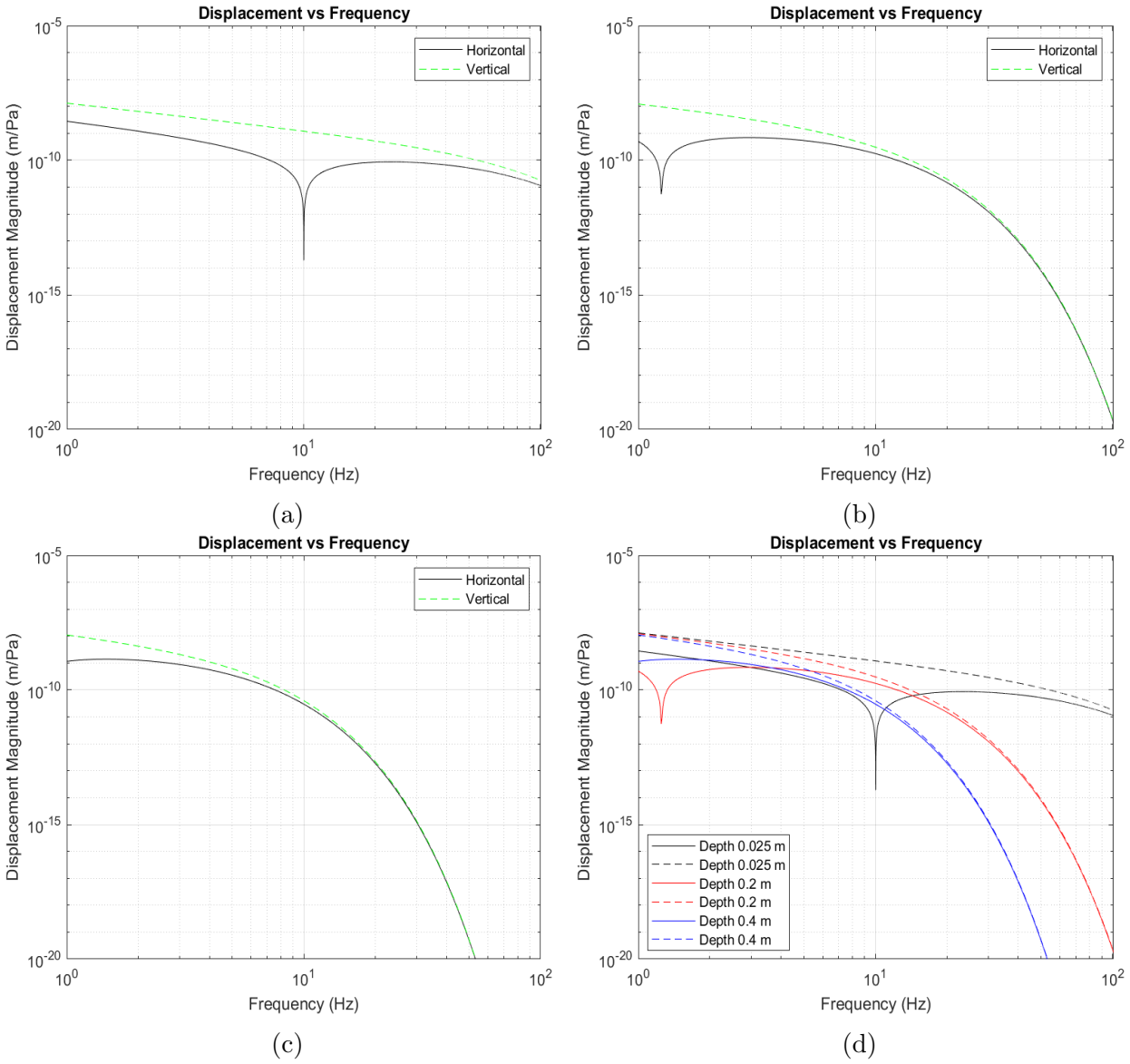

Figure 3: Effect of depth on horizontal and vertical component at (a) at 0.025 m (b) at depth of 0.2 m and (c) at depth of 0.4 m, for an average convective wind speed of 4.948 m/s. 4(d) represents (a), (b) and (c) in a single plot for comparison purpose.

4 Multi-Layer Models

4.1 Model II: Elastic Media over a Water Table

In an effort to improve the prediction of horizontal to vertical displacement ratio at lower frequency range, a more realistic ground model than an elastic half space is introduced. The water table is an underground boundary between the soil surface and the area where ground-water saturates spaces between sediments and cracks in rock. At this boundary, water pressure and atmospheric pressure are equal. The soil surface above the water table is called the unsaturated zone, where both oxygen and water fill the spaces between sediments. The shape and height of water table is influenced by the land surface that lies above it [12].

Model II consists of an elastic half space media, same as Naderyan's [9], over the water saturated layer. Table 2 shows value of various parameters as well as thickness *(d)* for layers. Shear and compression wave velocity for water-rich sediments are based on sample K019 [11].

Table 2: Model parameters for a multi-layer model II

ρ (kgm^{-3})	β (ms^{-1})	α (ms^{-1})	d (m)
1995	140	285	0.50
2000	541.60	1743.08	-

Figure 5 shows the displacement response as a function of frequency, at different depths, for the multi-layer model discussed above. The average convective velocity is taken as 4.948 m/s for this model as well. Comparison between Figure 3 and Figure 4 suggests that the response at higher frequencies is unaffected by the presence of the water table but shows an improved prediction at lower frequencies for sensors at 0.2 m and 0.4 m depth.

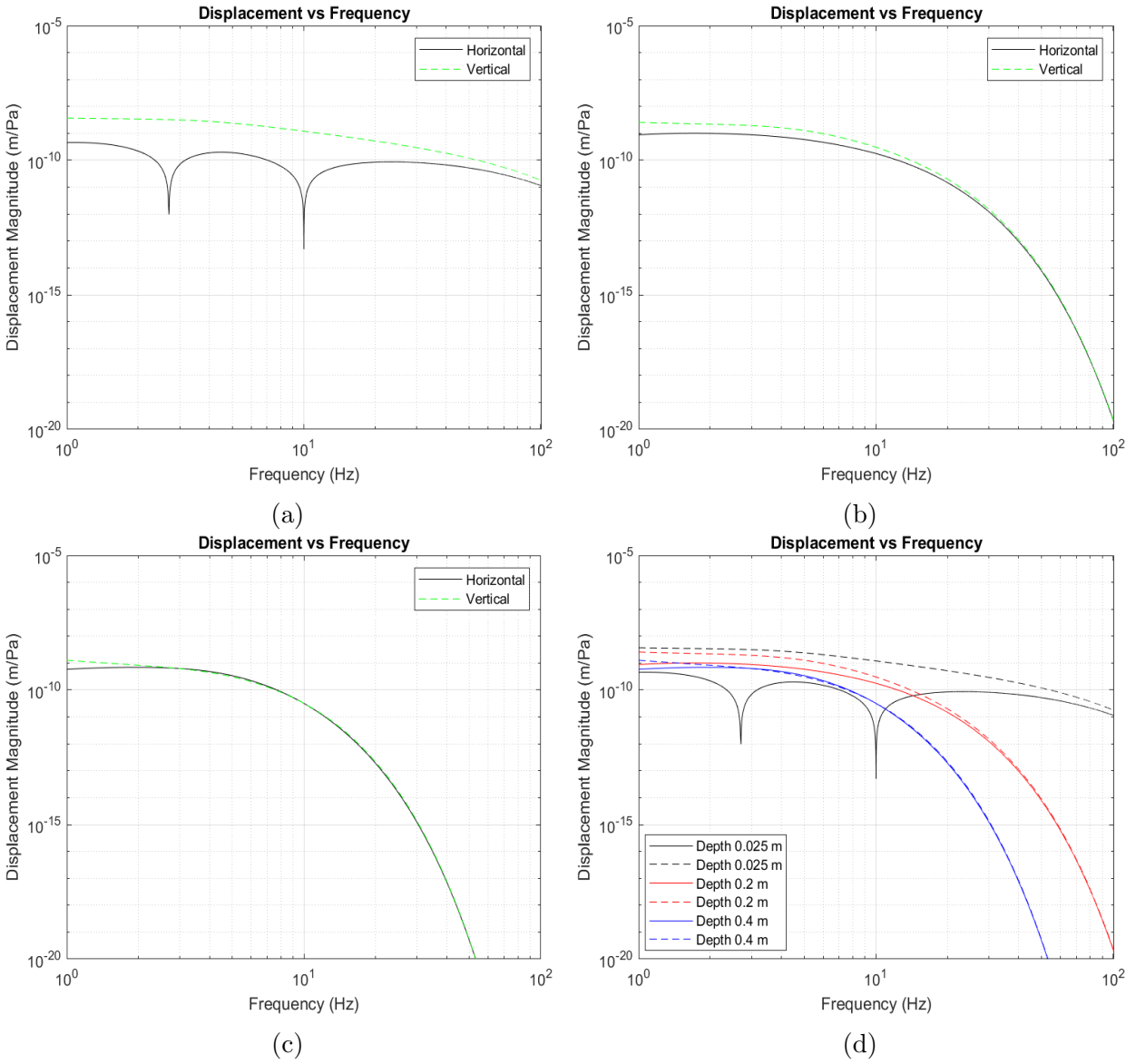

Figure 4: Effect of depth on horizontal and vertical component at (a) at 0.025 m (b) at depth of 0.2 m (c) at depth of 0.4 m, for an average convective wind speed of 4.948 m/s and (d) shows a cumulative plot.

Higher compression and shear velocities at depth may reduce vertical vs horizontal motion of ground because of less displacement at the interface between two layers. However, the presence of water table still shows a rapid attenuation of displacement behaviour with depth, which is not in agreement with experimental data shown by Nadeyran et al. [9].

4.2 Model III: Elastic Media Between a Thin Shear Layer and a Water Table

Model II showed an improvement in displacement ratio at lower frequencies. To model the ground more realistically, a thin top shear layer is introduced to Model II. In general, the top layer of the soil is associated with low shear speed. To model this, the shear speed of top layer soil with a thickness of 0.05 m is taken as 70 m/s which is half of the bulk value [5]. The middle layer has the same parameters as in the case of Model I and Model II.

Table 3 shows model parameters for an elastic media between a thin shear layer and a water table. Thickness of the middle layer is 0.45 m and water table acts as a half-space for Model III.

Table 3: Model parameters for a multi-layer model III

ρ (kgm^{-3})	β (ms^{-1})	α (ms^{-1})	d (m)
1900	70	240	0.05
1995	140	285	0.45
2000	541.60	1743.08	-

Figure 6 portrays the displacement response of Model III as a function of frequency at different depths for an average convective speed of 4.948 m/s. At lower frequency range, Model III shows an improvement in horizontal to vertical ratio especially for burial depth of 0.4 m. Displacement response for a sensor location at 0.2 m remains comparatively unchanged when compared with Figure 5(d). Ground motion at depth 0.025 shows a smooth response without the presence of dips. For most runs, a minima of the horizontal displacement was observed between 4-6 Hz.

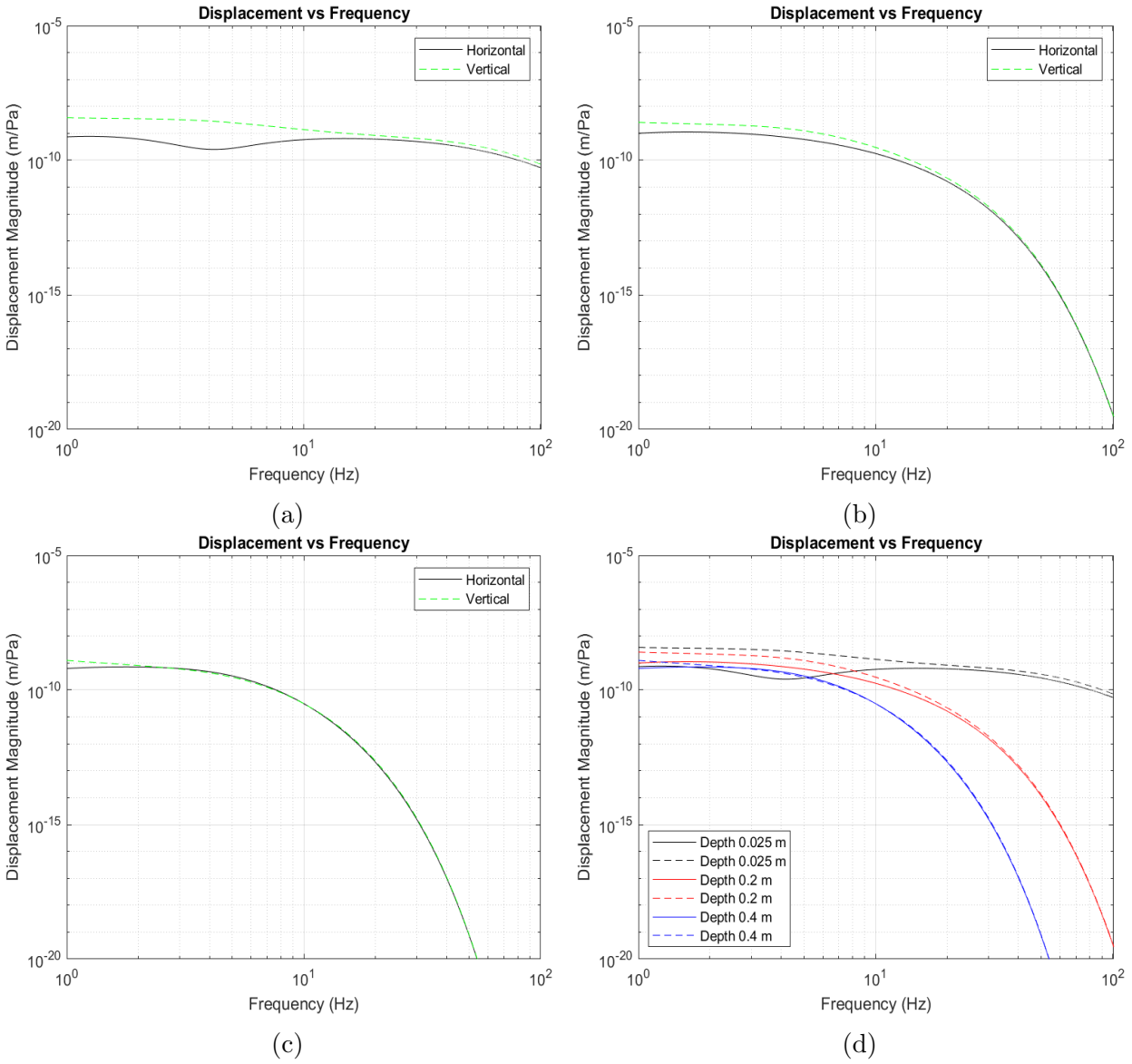

Figure 5: Effect of depth on horizontal and vertical component at (a) at 0.025 m (b) at depth of 0.2 m (c) at depth of 0.4 m, for an average convective wind speed of 4.948 m/s and (d) shows a cumulative plot.

4.3 Model IV: Inhomogeneous Media with Random Parameters

Ground does not exhibit uniform characteristics and is highly inhomogeneous and anisotropic in nature. Many studies have been conducted on inhomogeneous elastic media with random parameters in layers to investigate various phenomenon. Gilbert [3] used randomly layered

turbide model to study the reflection of sound from the ocean bottom. Similarly, Wheeler [5] also used a layered model to conduct sensitivity analysis to understand the effects of physical parameters on his modeled acoustic/seismic signature.

This section deals with the dynamic response of the ground due to pressure perturbations on the surface. This model is an extension of Model III, and consists of same thin shear top layer and water table as the bottom half-space. However, the middle layer is split into 10 discrete layers with randomly varying parameters. Random values for the model parameter follow normal distribution with mean values same as that of the middle layer in Model III. The degree of inhomogeneity in the discrete layers is introduced by setting different values of standard deviation σ for the normal distribution. Introducing such random layers to our model helps in predicting more accurate displacement response of the media and does a better work of physically representing the ground. We examine the effect of increasing inhomogeneity in ground to better understand the effects of the physical parameters on the Acoustic/Seismic coupling. Introducing such multiple layers with randomly varied parameters between a thin shear layer and a water table may reduce vertical with respect to horizontal because of interference of reflected waves from each layer.

Figure 6 shows a histogram plot of densities for various layers. Normal random distribution with a mean value of 1995 kg/m^3 and a standard deviation of 5 % is used to generate the plot. Similar procedure can be used to generate random values for compression wave speed, shear wave speed and layer thickness. Furthermore, the average for each components of displacement are obtained by dividing the total sum of values from each run by the number of runs. Thus, obtained mean values are plotted to show an average displacement for the vertical and horizontal components.

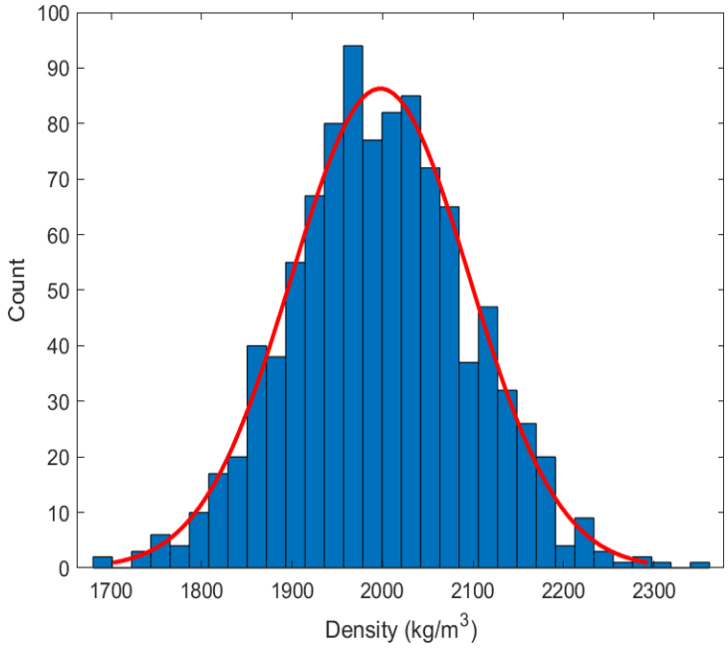

Figure 6: Histogram showing normal distribution of randomly generated values for density

4.3.1 Displacement Response at $\sigma = 5\%$

Figure 7 portrays displacement magnitude as a function of frequency at different depths and models that at a standard deviation of 5% from the corresponding mean parameter value (middle layer: Model III). The solid line in Figure 6 corresponds to horizontal component and dotted line corresponds to vertical component of displacement.

Since, every run of the program yields an unique result, Figure 7 compiles six plots for every run in one graph for a given depth and also shows an average of the six plots. Table 4 shows the mean and standard deviation used to generate normal distribution of random numbers for discrete layers.

Table 4: Basis for normal distribution of layer parameters for figure 6

	ρ (kgm^{-3})	β (ms^{-1})	α (ms^{-1})	d (m)
μ	1995	140	285	0.045
σ (5%)	99.75	7	14.25	0.00225

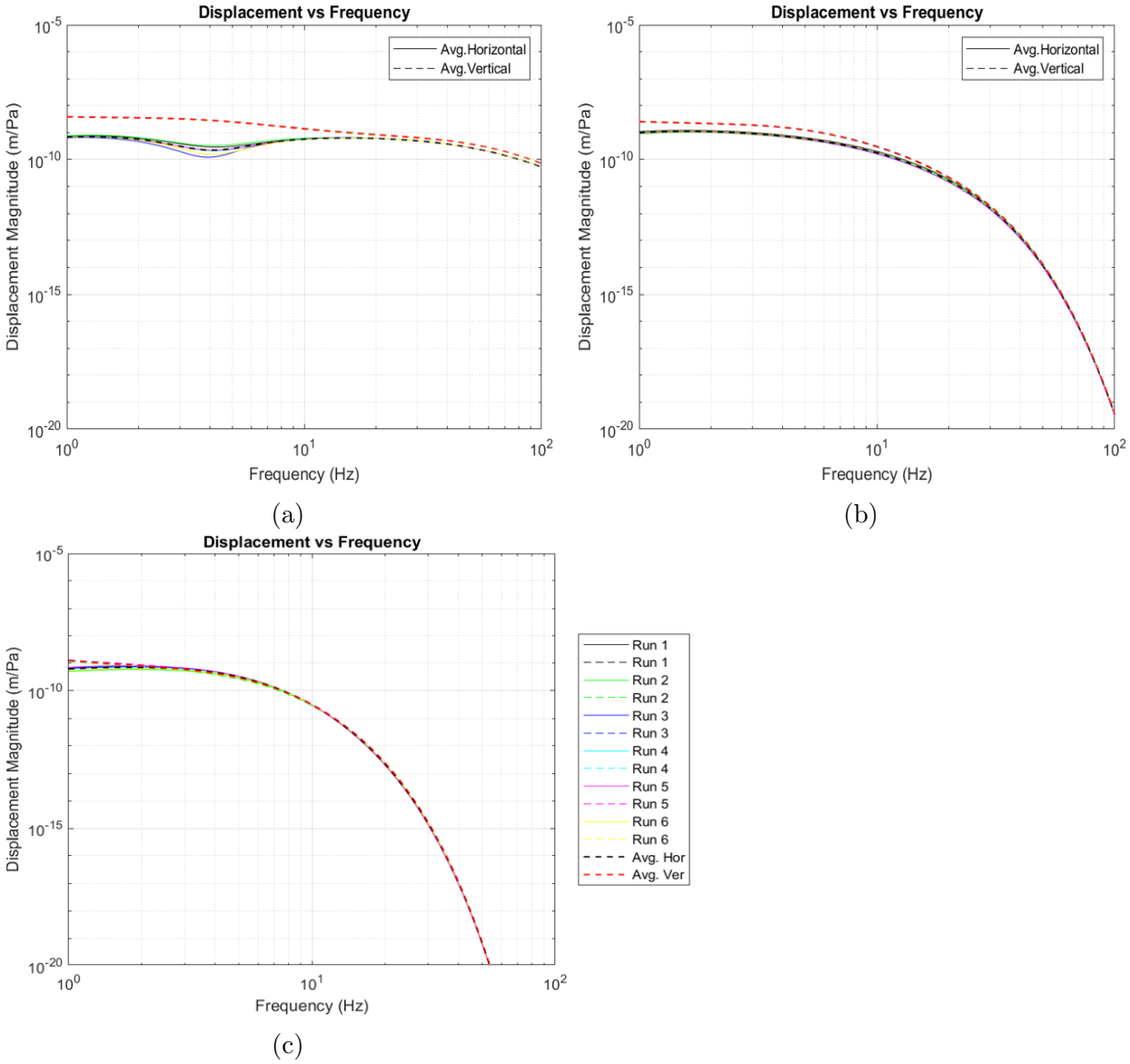

Figure 7: Effect of Inhomogeneity with $\sigma = 5\%$ on horizontal and vertical component at (a) at 0.025 m (b) at depth of 0.2 m and (c) at depth of 0.4 m, for an average wind speed of 4.948 m/s.

Introducing 5% inhomogeneity in the ground did not improve the prediction for the displacement response of the ground.

4.3.2 Displacement Response at $\sigma = 10\%$

We increase the degree of inhomogeneity to $\sigma = 10\%$ in subdivided layers to see if it makes the prediction for the displacement response agree with experimental data. Table 5 shows the tabulated data at $\sigma = 10\%$.

Table 5: Basis for normal distribution of layer parameters for figure 7

	ρ (kgm^{-3})	β (ms^{-1})	α (ms^{-1})	d (m)
μ	1995	140	285	0.045
σ (10%)	199.5	14	28.5	0.0045

Figure 8 captures the behavior of displacement response when the standard deviation for random normal distribution is increased. In comparison to $\sigma = 5\%$, the results in displacement response of inhomogeneous ground at $\sigma = 10\%$ indicate general similarities in their trends, and the measured amplitude attenuate at the same rate with the increase in frequency range. This behaviour is more apparent at depths of 0.2 m and 0.4 m than at flush mounted surface location. Increase in the degree of inhomogeneity to $\sigma = 10\%$ did not improve the predictions for displacement behaviour. However, occasional minima (dips) were observed in horizontal displacement component for lower frequencies at measurement depth of 0.025 m.

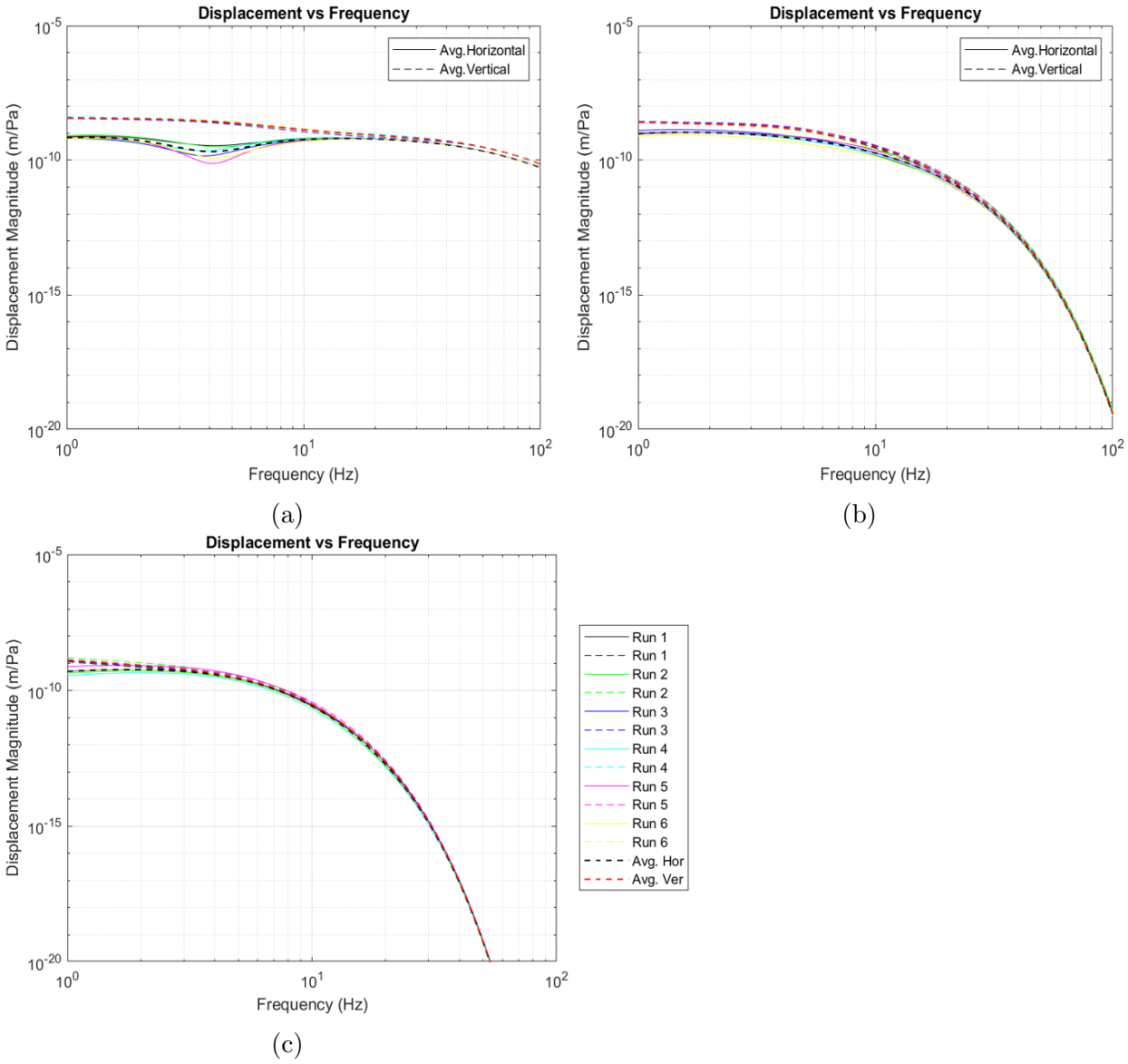

Figure 8: Effect of Inhomogeneity with $\sigma = 10\%$ on horizontal and vertical component at (a) at 0.025 m (b) at depth of 0.2 m and (c) at depth of 0.4 m, for an average wind speed of 4.948 m/s.

4.3.3 Displacement Response at $\sigma = 20\%$

When the layer parameters are varied at 20% above and below the base values, displacement response exhibit similar trend as in 4.3.1 and 4.3.2. However, multiple numeric simulation show that, at measurement depth of 2.5 cm, the horizontal component of displacement exhibit dips at lower frequency range. Table 6 reflects tabulated data of model parameters for discrete layers. Figure 9 suggests that, with the increase in depth, the displacement magnitudes are lowered at a given frequency.

Table 6: Basis for normal distribution of layer parameters for figure 8

	ρ (kgm^{-3})	β (ms^{-1})	α (ms^{-1})	d (m)
μ	1995	140	285	0.045
σ (20%)	399	28	57	0.009

Figure 9 shows the displacement behaviour of inhomogeneous ground at $\sigma = 20\%$. Even if the degree of inhomogeneity is increased, we do not observe any significant change in the horizontal component. For the measurement at 0.025 m depth, multiple dips in the horizontal are observed at lower frequencies as a result of phase change at those frequencies. Furthermore, the increase in inhomogeneity to 20% does not improve the prediction for the attenuation of ground motion with the increase in depth.

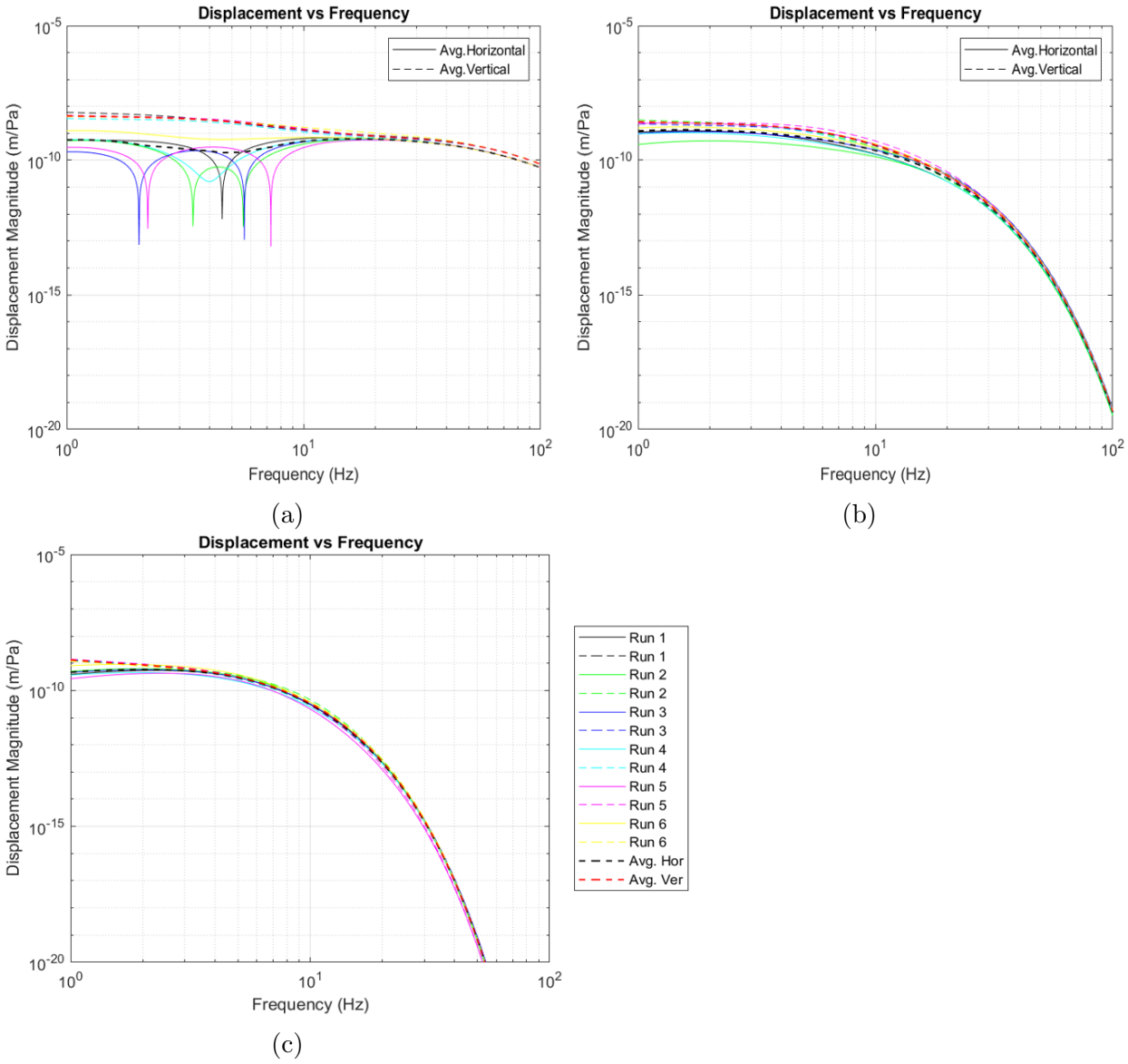

Figure 9: Effect of Inhomogeneity with $\sigma = 20\%$ on horizontal and vertical component at (a) at 0.025 m (b) at depth of 0.2 m and (c) at depth of 0.4 m, for an average wind speed of 4.948 m/s.

4.3.4 Displacement Response at $\sigma = 20\%$ with no variation in density

Often times variations in density above or below 20% of the mean ground model density is not realized. Therefore, we investigate the displacement behaviour of our inhomogeneous ground model at $\sigma = 20\%$ without any change in value for the density. Table 7 shows tabulated data of model parameters for discrete layers.

Table 7: Basis for normal distribution of layer parameters for Figure 9

	ρ (kgm^{-3})	β (ms^{-1})	α (ms^{-1})	d (m)
μ	1995	140	285	0.045
σ (20%)	0	28	57	0.009

Figure 10 shows the averaged behaviour of ground motion due to sinusoidal pressure fluctuation above the ground surface. Displacement behaviour remained fairly constant, especially at higher frequencies. In comparison to Figure 9 (a), Figure 10 (a) showed an improvement in prediction for horizontal component at lower frequencies for the measurement depth of 0.025 m. Furthermore, dips were not observed as often as for the varying density case.

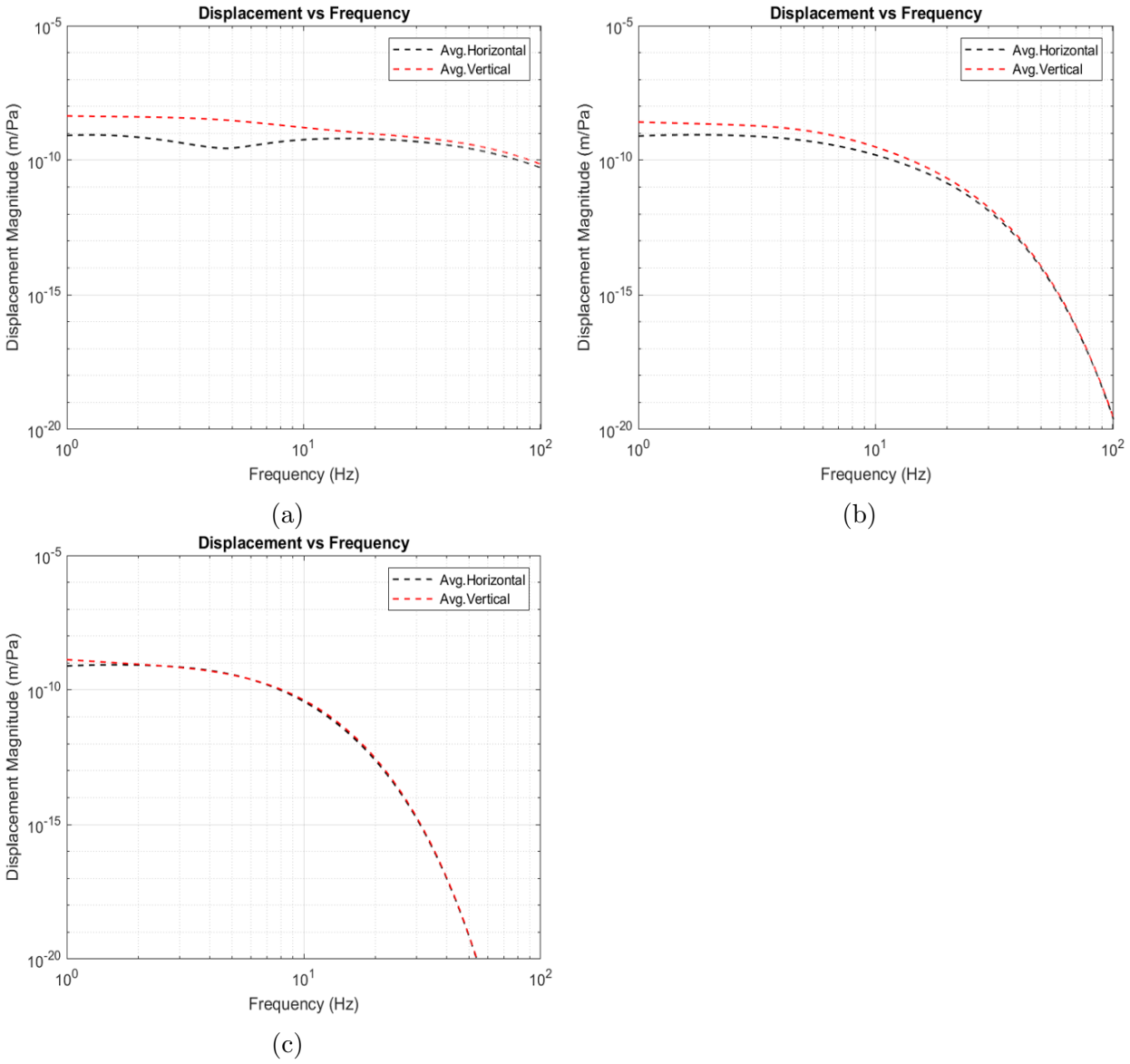

Figure 10: Effect of Inhomogeneity with $\sigma = 20\%$ on horizontal and vertical component at (a) at 0.025 m (b) at depth of 0.2 m and (c) at depth of 0.4 m, for an average wind speed of 4.948 m/s.

5 Conclusion

The quasi-static model used by Naderyan et al. [9] predicts that the vertical displacement is larger than the horizontal displacement and that the displacements decay rapidly with depth. The model did predict vertical ground displacements in good agreement with the measured vertical displacement. The horizontal ground displacements were significantly underpredicted and Naderyan et al. suggested that shear stress must be of the same order of magnitude of the normal pressure on the ground surface. Mohammadi[8] argues that the shear stresses are not large enough to account for the horizontal seismic wind noise data. In this study, a theoretical wave based approach - acoustic to seismic coupling, was adopted to predict the wind induced noise at different depths and frequencies. For better estimation of wind-noise, the ground was modeled as inhomogeneous elastic media that consists of a thin shear layer top surface followed by ten discrete layers with randomly varying layer parameters, which in turn followed by a bottom half space consisting of the water-saturated region known as the water table.

Naderyan's model shows displacement models are convergent at higher frequencies and that the ground motion had large decay with the increase in depths of measurement. The wave model based on Sorrells[13] predicts that vertical and horizontal displacements converge at higher frequencies but this is dependent on depth. A comparison between an elastic half space (Model I) and an elastic media with water table (Model II, III IV) suggests that introducing a water saturated layer as the bottom half space for Model I shows an improvement in horizontal to vertical displacement ratio at lower frequency range of 1-10 Hz. Higher compression and shear velocities at depth may reduce vertical vs horizontal motion of ground because of less displacement at the interface between the layers and the half space. For the frequency range of 1-10 Hz, at an average convective wind speed of 4.948 m/s, the horizontal component (Model II,III IV) is much lower than the vertical component for an elastic half-space over the same frequency range. Addition of water table

also decreases the vertical component of displacement slightly by a factor of 1.26 over the same frequency band. Furthermore, introducing a soft shear layer on top and a water table on the bottom of half space predicted the horizontal component very close to the vertical component at frequencies above 10 Hz, which is an improvement over Naderyan et al. [9] and Mohammadi [8]'s model. In the case of the inhomogeneous random layer model, increasing the degree of randomness in model parameters did not significantly affect the predictions for both components of displacement response of the ground. Acoustic to seismic coupling of ground model with a constant density for discrete layers and variable shear, compression wave velocities and depth also did not predict an improvement in horizontal displacement response at depth of 0.2 and 0.4 m.

When the measurement depth is increased, the vertical component and horizontal component attenuate rapidly and their ratio approaches closer to 1 beyond $\sim$ 50 Hz. It is also worth mentioning that results obtained from inhomogeneous stochastic layer model for the elastic media largely depend on the parameter values for each layer. Therefore, a large sample of data should be numerically computed in order to obtain accurate predictions on the displacement response of the in-homogeneous multi-layer model.

References

[1] Leonid Brekhovskikh. *Waves in layered media*. Trans. by Robert T. Beyer. Vol. 16, Chapter 1. Academic Press Inc., 1980.

[2] John W Dunkin. "Computation of modal solutions in layered, elastic media at high frequencies". *Bulletin of the Seismological Society of America* 55.2 (1965), pp. 335–358.

[3] Kenneth E Gilbert. "Reflection of sound from a randomly layered ocean bottom". *The Journal of the Acoustical Society of America* 68.5 (1980), pp. 1454–1458.

[4] Norman A Haskell. "The dispersion of surface waves on multilayered media". *Bulletin of the seismological Society of America* 43.1 (1953), pp. 17–34.

[5] Wheeler B. Howard. "Delineation of excessive strength soils through acoustic to seismic techniques". PhD thesis. The University of Mississippi, Jan. 2007.

[6] Daniel Lévesque and Luc Piché. "A robust transfer matrix formulation for the ultrasonic response of multilayered absorbing media". *The Journal of the Acoustical Society of America* 92.1 (1992), pp. 452–467.

[7] MATLAB. *version 9.7.0 (R2019b)*. Natick, Massachusetts: The MathWorks Inc., 2010.

[8] Mohammad Mohammadi. "Elastodynamic Model for Wind Induced Ground Motion". MA thesis. The University of Mississippi, Jan. 2018.

[9] Vahid Naderyan, Craig J Hickey, and Richard Raspet. "Wind-induced ground motion". *Journal of Geophysical Research: Solid Earth* 121.2 (2016), pp. 917–930.

[10] Raspet. R, Hickey. C.J., and Koirala. B. "Corrected tilt calculation for atmospheric pressure induced seismic noise". *Geophysical Journal International* (submitted January 5, 2021).

[11] Kai Schumann et al. “P and S wave velocity measurements of water-rich sediments from the Nankai Trough, Japan”. *Journal of Geophysical Research: Solid Earth* 119.2 (2014), pp. 787–805.

[12] National Geographic Society. *Water Table*. 2019. URL: https://www.nationalgeographic.org/encyclopedia/water-table.

[13] Gordon G Sorrells. “A preliminary investigation into the relationship between long-period seismic noise and local fluctuations in the atmospheric pressure field”. *Geophysical Journal International* 26.1-4 (1971), pp. 71–82.

[14] William T Thomson. “Transmission of elastic waves through a stratified solid medium”. *Journal of Applied Physics* 21.2 (1950), pp. 89–93.